Supporting Information for:

Nano-FTIR Spectroscopy of the Solid Electrolyte Interphase Layer on a Thin-Film Silicon Li-ion Anode

Andrew Dopilka[1 *], Yueran Gu[1,2], Jonathan M. Larson[1], Vassilia Zorba[1,2], Robert Kostecki[1 *]

[1]Energy Storage and Distributed Resources Division, Lawrence Berkeley National Laboratory, Berkeley, CA 94720, USA

[2]Department of Mechanical Engineering, University of California, Berkeley, CA 94720, USA

Corresponding Author*
Andrew Dopilka adopilka@lbl.gov
Robert Kostecki r_kostecki@lbl.gov

Figures

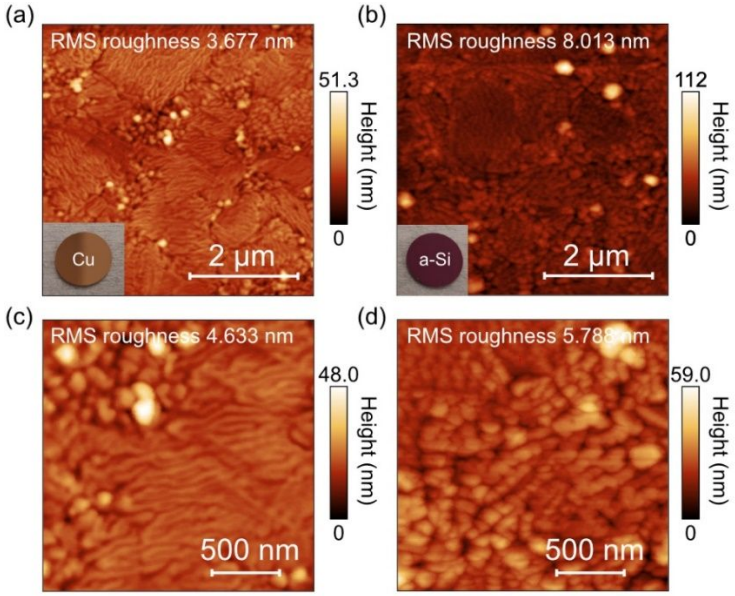

Figure S1 AFM topography of the as sputtered **(a)(c)** Cu electrode and **(b)(d)** amorphous Si (a-Si) electrodes. The insets include the RMS roughness and photographs of the ½ inch diameter electrodes.

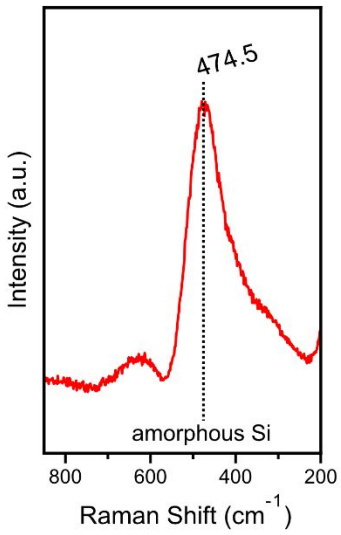

Figure S2 Raman spectrum of the sputtered a-Si film showing the broad peak characteristic of amorphous Si. The raman spectroscopy was performed with a Renishwa inVia Raman Microscope.

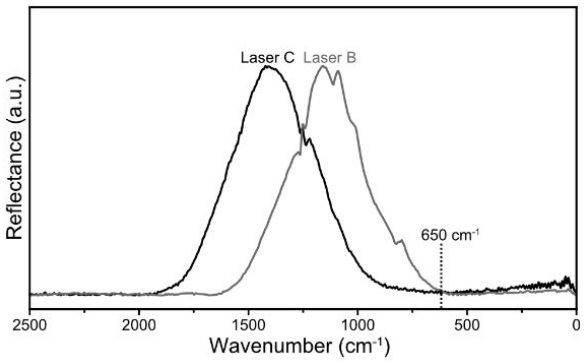

Figure S3 Near-field reflectance spectra of the IR lasers on a Si wafer used in this work. These wavenumber distributions demonstrate the wavenumber range used to measure the IR absorption of the SEI layer.

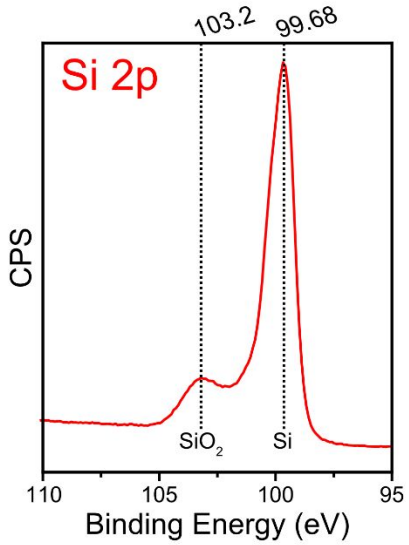

Figure S4 High resolution XPS spectrum of the Si 2p region of the pristine a-Si electrode.

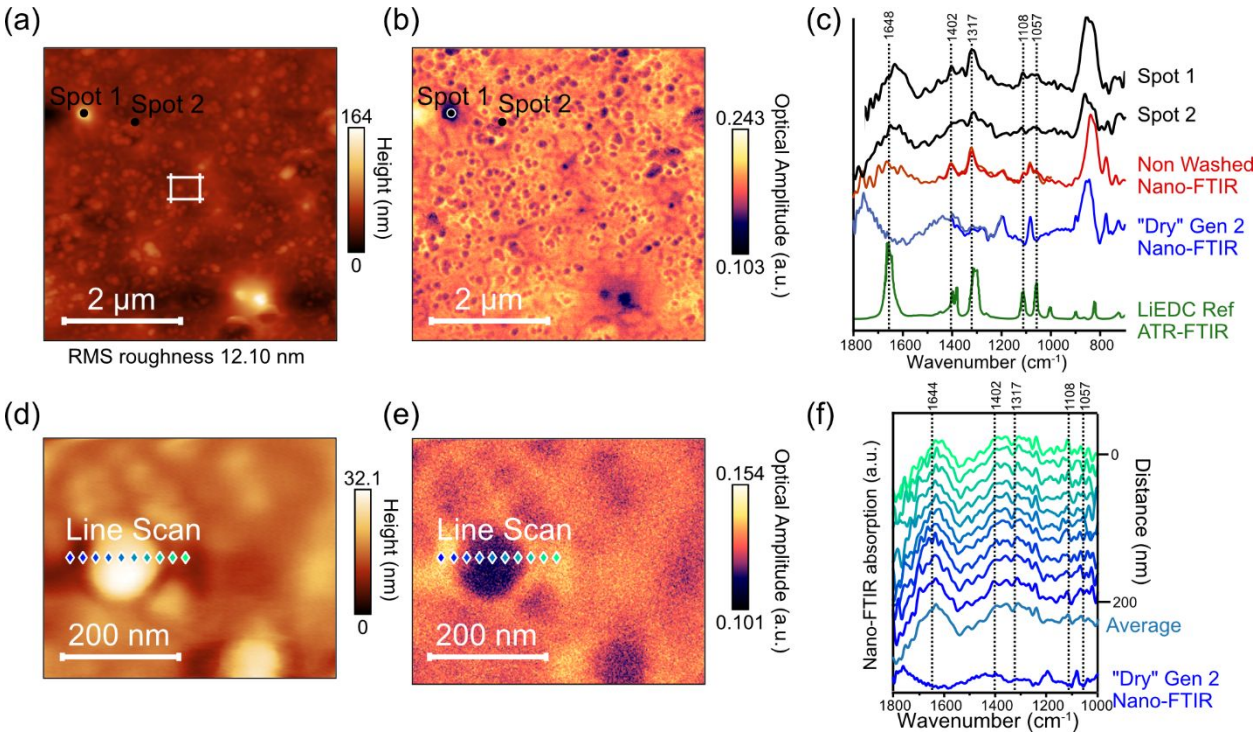

Figure S5 5 x 5 µm AFM topography (**a**), and near-field white light image (**b**) of the washed (after 5 second immersion in DMC) a-Si electrode after the 5 CV cycles and 12 hour 0.05 V hold. Nano-FTIR spectra at two spots marked in images (a) and (b) compared with the non-washed nano-FTIR spectra, "dry" Gen 2 electrolyte and LiEDC reference spectra (**c**). 0.5 x 0.4 µm AFM topography (**d**) and near-field whitelight image (**e**) of the washed electrode. Nano-FTIR spectra from the line scan at the locations marked in images (d) and (e) (**f**).

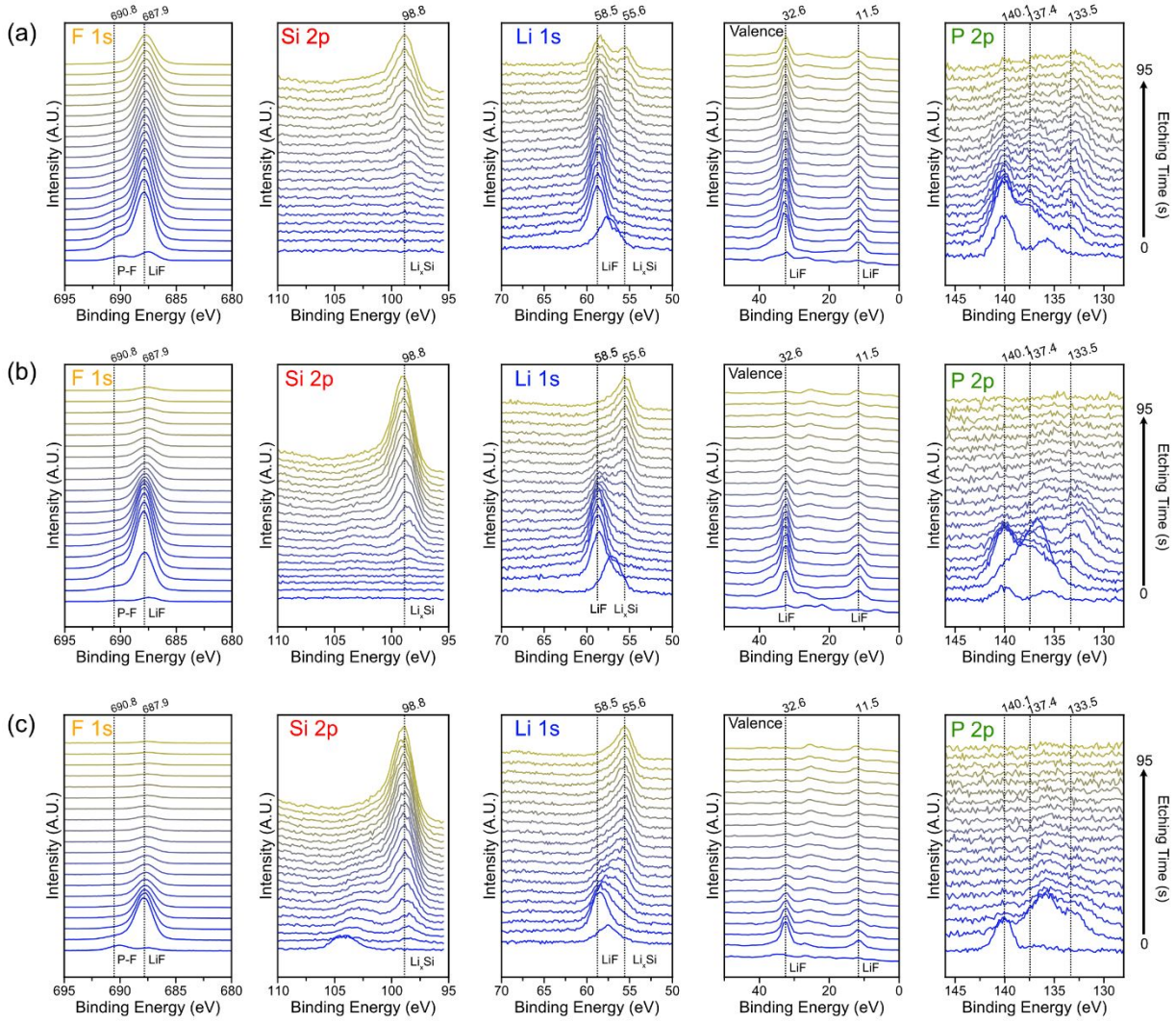

Figure S6 High resolution XPS spectra of F 1s, Si 2p, Li 1s, valence[1], and P 2p for the a-Si electrodes after 5 CV cycles and a 12 hour hold at 0.05 V that were **(a)** non-washed, **(b)** washed for 1 s with 50 uL of DMC, and **(c)** immersed in 5 mL of DMC for 5 s.

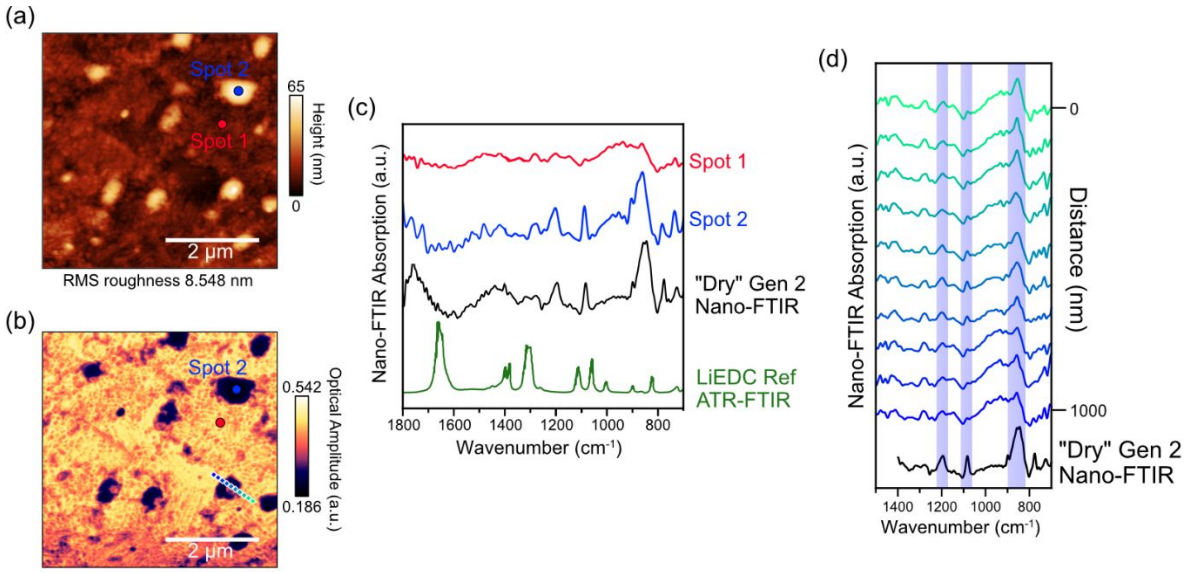

Figure S7 AFM topography **(a)** and near-field white light image **(b)** of the non-washed a-Si electrode scanned from OCV to 0.5 V at 0.1 mV/s. Nano-FTIR spectra from two locations shown in (a) compared with the "Dry" Gen 2 electrolyte and LiEDC reference spectra (**c**). Nano-FTIR spectra from the line scan at the locations marked in image (b) **(d)**.

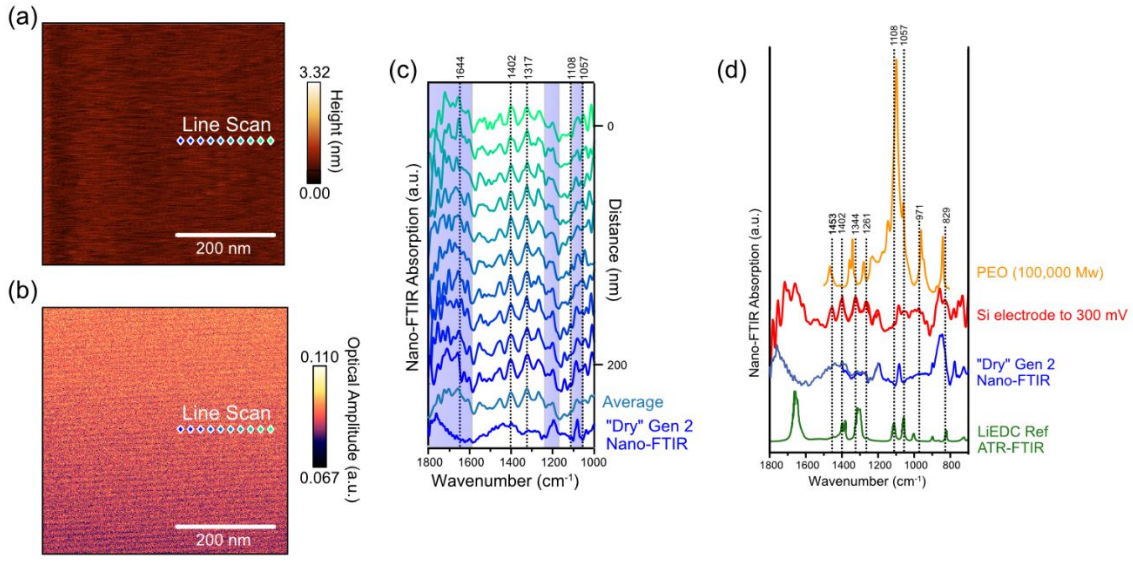

Figure S8 AFM topography **(a)** and near-field white light image **(b)** of the non-washed a-Si electrode scanned from OCV to 0.3 V at 0.1 mV/s. Nano-FTIR spectra from the line scan at the locations marked in the AFM and white light images (a) and (b) compared with the spectrum of "Dry" Gen 2 electrolyte **(c)**. Comparison of the nano-FTIR spectra obtained at 0.3 V to the ATR-FTIR spectra of PEO (100,000 molecular weight (Mw) from ref[2]), "Dry" Gen 2 electrolyte and LiEDC.

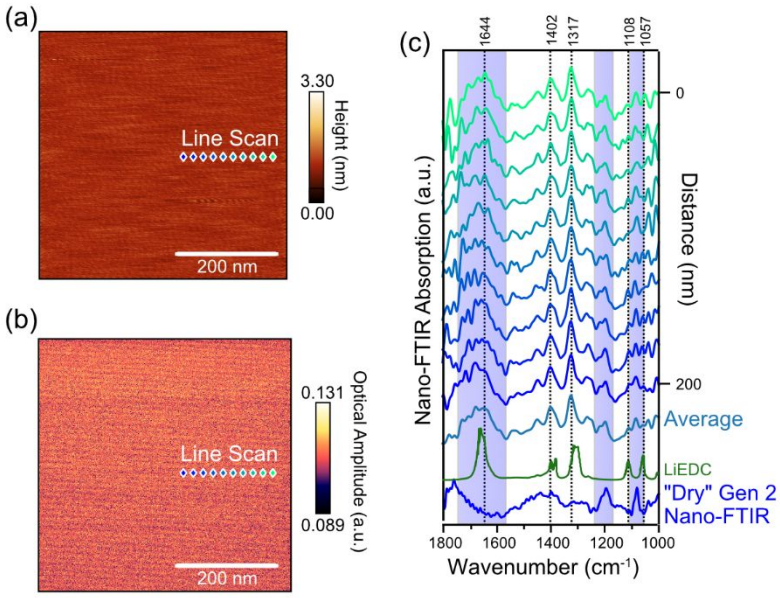

Figure S9 AFM topography **(a)** and near-field white light image **(b)** of the non-washed a-Si electrode scanned from OCV to 0.05 V at 0.1 mV/s. Nano-FTIR spectra from the line scan at the locations marked in the AFM and white light images compared with the "Dry" Gen 2 electrolyte and LiEDC reference **(c)**.

Tables

Table S1. Review of the washing procedures reported in the literature for studying the SEI on Si anodes

Si Material	Washing time/Method	Washing Solvent	Washing Amount	Ref
50 nm a-Si on Cu foil	5 s	DMC	N/A	[3]
Si wafer	1-2 minutes	DMC	1 mL	[4]
Si Wafer	Rinsed twice	DMC	N/A	[5]
50 nm a-Si on Cu foil	Gently Rinsed in Triplicate, removed with kimwipe	DEC	N/A	[6]
Si wafer	Soaked three times	DEC	N/A	[7,8]
Si wafer	2 minutes	DMC	N/A	[9]
Binder free Si nanoparticle electrode	N/A	DMC	N/A	[10]
a-Si thin film on Cu foil (neutron)	N/A	DMC	2 mL	[11]
Si on Cu grid	N/A	DEC	50 uL	[12]
Si wafer	2 min	DMC	N/A	[13]
Si composite electrode	N/A Sonicating electrode	DMC	N/A	[14]
Si composite electrode	Three successive baths, 1 minute each	DMC	2 mL bath	[15,16]
Si wafer	Washed three times	DEC	~5 mL each time	[17]
a-Si thin film on Cu	10 s	DEC	200 uL	[18]
Si nanowires	Rinse three times	DMC	N/A	[19]

Binder free silicon electrode	Rinsed four times	DMC	1 mL (in total)	[20]
Si composite electrode	Rinsed three times	DMC	N/A	[21]
Porous Si composite electrode	Softly washed three times	DMC	N/A	[22]
Si thin film	Soaked	Protonated DMC	N/A	[23]
Si nanowires	Overnight	DMC	N/A	[24]
Si nanoparticle electrode	Carefully rinsed 4 times	DMC	1 mL (in total)	[25]
Si Wafer	60 s	DMC	1 mL	[26]
Si thin film	N/A	DMC	N/A	[27]
Si composite electrode	N/A	DMC	N/A	[28]
Si thin film	60 s	DMC	1 mL	[29]
Si Wafer	N/A	DMC	N/A	[30]
Thin film Si	Rinsed four times	DEC	N/A	[31]
Si nanoparticles composite electrode	N/A	DEC	N/A	[32]
Si thin film	Gently rinsed	DMC	N/A	[33]
Si Thin film	Gently rinsed	DMC	N/A	[34]
Si wafer	Washed three times	DEC/PC	1-3 mL	[35]
Si nanoparticle composite electrode	N/A	DMC	N/A	[36]
Si thin film/Si nanowires	N/A	DMC	N/A	[37]

References

(1) Dedryvère, R.; Martinez, H.; Leroy, S.; Lemordant, D.; Bonhomme, F.; Biensan, P.; Gonbeau, D. Surface Film Formation on Electrodes in a LiCoO2/Graphite Cell: A Step by Step XPS Study. *J Power Sources* **2007**, *174*, 462–468.

(2) He, X.; Larson, J. M.; Bechtel, H. A.; Kostecki, R. In Situ Infrared Nanospectroscopy of the Local Processes at the Li/Polymer Electrolyte Interface. *Nat Commun* **2022**, *13*.

(3) Schnabel, M.; Lin, T. C.; Arca, E.; Yoon, I.; Veith, G. M.; He, X.; Kostecki, R. Stable SEI Formation on Al-Si-Mn Metallic Glass Li-Ion Anode. *J Electrochem Soc* **2021**, *168*, 100521.

(4) Schnabel, M.; Arca, E.; Ha, Y.; Stetson, C.; Teeter, G.; Han, S. D.; Stradins, P. Enhanced Interfacial Stability of Si Anodes for Li-Ion Batteries via Surface SiO2Coating. *ACS Appl Energy Mater* **2020**, *3*, 8842–8849.

(5) Cao, C.; Abate, I. I.; Sivonxay, E.; Shyam, B.; Jia, C.; Moritz, B.; Devereaux, T. P.; Persson, K. A.; Steinrück, H. G.; Toney, M. F. Solid Electrolyte Interphase on Native Oxide-Terminated Silicon Anodes for Li-Ion Batteries. *Joule* **2019**, *3*, 762–781.

(6) Nanda, J.; Yang, G.; Hou, T.; Voylov, D. N.; Li, X.; Ruther, R. E.; Naguib, M.; Persson, K.; Veith, G. M.; Sokolov, A. P. Unraveling the Nanoscale Heterogeneity of Solid Electrolyte Interphase Using Tip-Enhanced Raman Spectroscopy. *Joule* **2019**, *3*, 2001–2019.

(7) Vogl, U. S.; Lux, S. F.; Crumlin, E. J.; Liu, Z.; Terborg, L.; Winter, M.; Kostecki, R. The Mechanism of SEI Formation on a Single Crystal Si(100) Electrode. *J Electrochem Soc* **2015**, *162*, A603–A607.

(8) Vogl, U. S.; Lux, S. F.; Das, P.; Weber, A.; Placke, T.; Kostecki, R.; Winter, M. The Mechanism of SEI Formation on Single Crystal Si(100), Si(110) and Si(111) Electrodes. *J Electrochem Soc* **2015**, *162*, A2281–A2288.

(9) Yin, Y.; Arca, E.; Wang, L.; Yang, G.; Schnabel, M.; Cao, L.; Xiao, C.; Zhou, H.; Liu, P.; Nanda, J.; et al. Nonpassivated Silicon Anode Surface. *ACS Appl Mater Interfaces* **2020**, *12*, 26593–26600.

(10) Nie, M.; Abraham, D. P.; Chen, Y.; Bose, A.; Lucht, B. L. Silicon Solid Electrolyte Interphase (SEI) of Lithium Ion Battery Characterized by Microscopy and Spectroscopy. *Journal of Physical Chemistry C* **2013**, *117*, 13403–13412.

(11) Fears, T. M.; Doucet, M.; Browning, J. F.; Baldwin, J. K. S.; Winiarz, J. G.; Kaiser, H.; Taub, H.; Sacci, R. L.; Veith, G. M. Evaluating the Solid Electrolyte Interphase Formed on Silicon Electrodes: A Comparison of: Ex Situ X-Ray Photoelectron Spectroscopy and in Situ Neutron Reflectometry. *Physical Chemistry Chemical Physics* **2016**, *18*, 13927–13940.

(12) Huang, W.; Wang, J.; Braun, M. R.; Zhang, Z.; Li, Y.; Boyle, D. T.; McIntyre, P. C.; Cui, Y. Dynamic Structure and Chemistry of the Silicon Solid-Electrolyte Interphase Visualized by Cryogenic Electron Microscopy. *Matter* **2019**, *1*, 1232–1245.

(13) Stetson, C.; Yin, Y.; Norman, A.; Harvey, S. P.; Schnabel, M.; Ban, C.; Jiang, C. S.; DeCaluwe, S. C.; Al-Jassim, M. Evolution of Solid Electrolyte Interphase and Active Material in the Silicon Wafer Model System. *J Power Sources* **2021**, *482*.

(14) Zhang, Y.; Li, X.; Sivonxay, E.; Wen, J.; Persson, K. A.; Vaughey, J. T.; Key, B.; Dogan, F. Silicon Anodes with Improved Calendar Life Enabled By Multivalent Additives. *Adv Energy Mater* **2021**, *11*.

(15) Philippe, B.; Dedryvère, R.; Allouche, J.; Lindgren, F.; Gorgoi, M.; Rensmo, H.; Gonbeau, D.; Edström, K. Nanosilicon Electrodes for Lithium-Ion Batteries: Interfacial Mechanisms Studied by Hard and Soft X-Ray Photoelectron Spectroscopy. *Chemistry of Materials* **2012**, *24*, 1107–1115.

(16) Philippe, B.; Dedryveère, R.; Gorgoi, M.; Rensmo, H.; Gonbeau, D.; Edström, K. Role of the LiPF6 Salt for the Long-Term Stability of Silicon Electrodes in Li-Ion Batteries - A Photoelectron Spectroscopy Study. *Chemistry of Materials* **2013**, *25*, 394–404.

(17) Schroder, K. W.; Celio, H.; Webb, L. J.; Stevenson, K. J. Examining Solid Electrolyte Interphase Formation on Crystalline Silicon Electrodes: Influence of Electrochemical Preparation and Ambient Exposure Conditions. *Journal of Physical Chemistry C* **2012**, *116*, 19737–19747.

(18) Hasa, I.; Haregewoin, A. M.; Zhang, L.; Tsai, W. Y.; Guo, J.; Veith, G. M.; Ross, P. N.; Kostecki, R. Electrochemical Reactivity and Passivation of Silicon Thin-Film Electrodes in Organic Carbonate Electrolytes. *ACS Appl Mater Interfaces* **2020**, *12*, 40879–40890.

(19) He, Y.; Jiang, L.; Chen, T.; Xu, Y.; Jia, H.; Yi, R.; Xue, D.; Song, M.; Genc, A.; Bouchet-Marquis, C.; et al. Progressive Growth of the Solid–Electrolyte Interphase towards the Si Anode Interior Causes Capacity Fading. *Nat Nanotechnol* **2021**, *16*, 1113–1120.

(20) Young, B. T.; Heskett, D. R.; Nguyen, C. C.; Nie, M.; Woicik, J. C.; Lucht, B. L. Hard X-Ray Photoelectron Spectroscopy (HAXPES) Investigation of the Silicon Solid Electrolyte Interphase (SEI) in Lithium-Ion Batteries. *ACS Appl Mater Interfaces* **2015**, *7*, 20004–20011.

(21) Chen, X.; Li, X.; Mei, D.; Feng, J.; Hu, M. Y.; Hu, J.; Engelhard, M.; Zheng, J.; Xu, W.; Xiao, J.; et al. Reduction Mechanism of Fluoroethylene Carbonate for Stable Solid-Electrolyte Interphase Film on Silicon Anode. *ChemSusChem* **2014**, *7*, 549–554.

(22) Li, Q.; Liu, X.; Han, X.; Xiang, Y.; Zhong, G.; Wang, J.; Zheng, B.; Zhou, J.; Yang, Y. Identification of the Solid Electrolyte Interface on the Si/C Composite Anode with FEC as the Additive. *ACS Appl Mater Interfaces* **2019**, *11*, 14066–14075.

(23) Veith, G. M.; Doucet, M.; Baldwin, J. K.; Sacci, R. L.; Fears, T. M.; Wang, Y.; Browning, J. F. Direct Determination of Solid-Electrolyte Interphase Thickness and Composition as a Function of State of Charge on a Silicon Anode. *Journal of Physical Chemistry C* **2015**, *119*, 20339–20349.

(24) Chan, C. K.; Ruffo, R.; Hong, S. S.; Cui, Y. Surface Chemistry and Morphology of the Solid Electrolyte Interphase on Silicon Nanowire Lithium-Ion Battery Anodes. *J Power Sources* **2009**, *189*, 1132–1140.

(25) Nguyen, C. C.; Yoon, T.; Seo, D. M.; Guduru, P.; Lucht, B. L. Systematic Investigation of Binders for Silicon Anodes: Interactions of Binder with Silicon Particles and Electrolytes and Effects of Binders on Solid Electrolyte Interphase Formation. *ACS Appl Mater Interfaces* **2016**, *8*, 12211–12220.

(26) Ha, Y.; Stetson, C.; Harvey, S. P.; Teeter, G.; Tremolet De Villers, B. J.; Jiang, C. S.; Schnabel, M.; Stradins, P.; Burrell, A.; Han, S. D. Effect of Water Concentration in LiPF6-Based Electrolytes on the Formation, Evolution, and Properties of the Solid Electrolyte Interphase on Si Anodes. *ACS Appl Mater Interfaces* **2020**, *12*, 49563–49573.

(27) Nakai, H.; Kubota, T.; Kita, A.; Kawashima, A. Investigation of the Solid Electrolyte Interphase Formed by Fluoroethylene Carbonate on Si Electrodes. *J Electrochem Soc* **2011**, *158*, A798–A801.

(28) Hopkins, E. J.; Frisco, S.; Pekarek, R. T.; Stetson, C.; Huey, Z.; Harvey, S.; Li, X.; Key, B.; Fang, C.; Liu, G.; et al. Examining CO 2 as an Additive for Solid Electrolyte Interphase Formation on Silicon Anodes . *J Electrochem Soc* **2021**, *168*, 030534.

(29) Veith, G. M.; Doucet, M.; Sacci, R. L.; Vacaliuc, B.; Baldwin, J. K.; Browning, J. F. Determination of the Solid Electrolyte Interphase Structure Grown on a Silicon Electrode Using a Fluoroethylene Carbonate Additive. *Sci Rep* **2017**, *7*.

(30) Stetson, C.; Schnabel, M.; Li, Z.; Harvey, S. P.; Jiang, C. S.; Norman, A.; Decaluwe, S. C.; Al-Jassim, M.; Burrell, A. Microscopic Observation of Solid Electrolyte Interphase Bilayer Inversion on Silicon Oxide. *ACS Energy Lett* **2020**, *5*, 3657–3662.

(31) Xie, H.; Sayed, S. Y.; Kalisvaart, W. P.; Schaper, S. J.; Müller-Buschbaum, P.; Luber, E. J.; Olsen, B. C.; Haese, M.; Buriak, J. M. Adhesion and Surface Layers on Silicon Anodes Suppress Formation of C-Li3.75Si and Solid-Electrolyte Interphase. *ACS Appl Energy Mater* **2020**, *3*, 1609–1616.

(32) Sina, M.; Alvarado, J.; Shobukawa, H.; Alexander, C.; Manichev, V.; Feldman, L.; Gustafsson, T.; Stevenson, K. J.; Meng, Y. S. Direct Visualization of the Solid Electrolyte Interphase and Its Effects on Silicon Electrochemical Performance. *Adv Mater Interfaces* **2016**, *3*.

(33) Nadimpalli, S. P. V.; Sethuraman, V. A.; Dalavi, S.; Lucht, B.; Chon, M. J.; Shenoy, V. B.; Guduru, P. R. Quantifying Capacity Loss Due to Solid-Electrolyte-Interphase Layer Formation on Silicon Negative Electrodes in Lithium-Ion Batteries. *J Power Sources* **2012**, *215*, 145–151.

(34) Li, Z.; Stetson, C.; Teeter, G.; Norman, A.; Ha, Y.; Tremolet De Villers, B. J.; Huey, Z.; Walker, P.; Han, S. D.; Decaluwe, S. C.; et al. Improving Interface Stability of Si Anodes by Mg Coating in Li-Ion Batteries. *ACS Appl Energy Mater* **2020**, *3*, 11534–11539.

(35) Schroder, K. W.; Dylla, A. G.; Harris, S. J.; Webb, L. J.; Stevenson, K. J. Role of Surface Oxides in the Formation of Solid-Electrolyte Interphases at Silicon Electrodes for Lithium-Ion Batteries. *ACS Appl Mater Interfaces* **2014**, *6*, 21510–21524.

(36) Zhang, X.; Weng, S.; Yang, G.; Li, Y.; Li, H.; Su, D.; Gu, L.; Wang, Z.; Wang, X.; Chen, L. Interplay between Solid-Electrolyte Interphase and (in)Active LixSi in Silicon Anode. *Cell Rep Phys Sci* **2021**, *2*.

(37) Pereira-Nabais, C.; Światowska, J.; Chagnes, A.; Ozanam, F.; Gohier, A.; Tran-Van, P.; Cojocaru, C. S.; Cassir, M.; Marcus, P. Interphase Chemistry of Si Electrodes Used as Anodes in Li-Ion Batteries. *Appl Surf Sci* **2013**, *266*, 5–16.